Journal of Engineering Physics and Thermophysics, Vol. 81, No. 5, 2008

MISCELLANEOUS

DESIGN OF SEMICONDUCTOR MATERIALS FOR ELECTRONICS. SEGMENT OF THE TECHNOLOGICAL PROCESS: ANNEALING OF THE BASE SUBSTRATE AND FORMATION OF A NANOSTRUCTURE OF DOPANTS

G. A. Tarnavskii

UDC 519.2:541.1

For one production segment of designing semiconductor materials with given electrophysical properties, computer simulation of a number of basic technological physicochemical processes has been performed. With the use of high-resolution algorithms, the dynamics of thermal oxidation of the base material (silicon) and the evolution of the SiO_2/Si and SiO_2/O_2 oxide film interfaces have been investigated. Simulation of the process of segregation of the acceptor and donor dopants (boron and phosphorus) in the base material at the SiO_2/Si oxidation wave front has been performed. For the "trench"-type geometry of the substrate surface, the distributions of boron and phosphorus concentrations have been obtained. It has been shown that the uniform (at the initial instant of time) distribution of dopant concentrations in the base material transforms to a distribution of narrowly-localized (of width about 65 nm) high-intensity peaks. Such nanostructures of donor and acceptor impurities in the substrate provide the required semiconductor electrophysical properties of the material.

Introduction. Designing of integrated circuits is based on the creation on the surface of monocrystalline silicon (base substrate) of sequential layers with different electrophysical properties. The number of these layers depends on the design-project of a particular integrated circuit being developed. The production of modern materials, in particular, for microprocessors, is based on MOS ("metal–oxide–semiconductor") technologies and represents a multistep production cycle consisting of 300-plus stages — segments (see, e.g., [1]). Each of these segments uses various complex physicochemical and mechanical processes. Of these, the two main processes are the process of oxidation of the base material (transformation of silicon Si to silicon dioxide SiO_2) and the process of segregation of dopants implanted in the base material at the SiO_2/Si oxidation wave front.

Physico-Mathematical Formulation and Parameters of Computer Simulation of the Technological Process. Computer simulation is used in investigating the physicochemical processes of one of the technological stages frequently used in the production cycle. Doping agents of the acceptor and donor type (B and P) are implanted in the base substrate of crystalline silicon. On the silicon surface a "trench"-type rectangular groove is cut. Figure 1 presents the configuration and dimensions of the region at the initial instant of time (the dimensions are given in micrometers).

The calculation region is divided into two parts — the subregion of the material Si and the subregion of the oxidizer — oxygen O_2. Between them a third part is situated — the subregion of the oxide SiO_2 which at the initial instant of time is a very thin film the dynamics of whose development is one of the goals of the investigation. The boundary between the subregions is given by a solid line and consists of five parts: the left and right horizontal surfaces, the left and right vertical walls of the "trench" of different height, and its bottom. Part of the material surface is covered with three nitride masks Si_3N_4 impenetrable for O_2 and protecting the corresponding surfaces of Si from direct oxidation (only oxidation resulting from the penetration of O_2 through the mask material takes place). The

Institute of Computational Mathematics and Mathematical Geophysics, Siberian branch of the Russian Academy of Sciences, 6 Lavrent'ev Ave., Novosibirsk, 630060, Russia; email: Gennady.Tarnavsky@gmail.com. Translated from Inzhenerno-Fizicheskii Zhurnal, Vol. 81, No. 5, pp. 994–1004, September–October, 2008. Original article submitted October 5, 2006; revision submitted November 14, 2007.

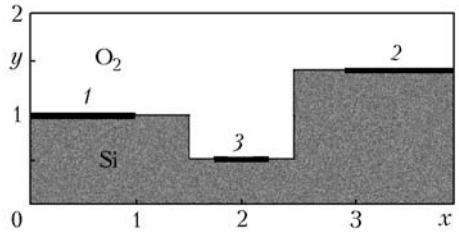

Fig. 1. Topology of the investigated region: initial configuration of the material Si and oxidizer O_2 boundary and arrangement of Si_3N_4 protective masks (1, 2, 3).

masks are marked in Fig. 1 by semiboldface lines. The concrete coordinates of the surface and protective masks are also given in the figure.

We consider the processes of Si oxidation with the determination of the configuration and dynamics of the SiO_2/Si and SiO_2/O_2 interfaces and the segregation of dopants B and P at the SiO_2 front. The dimensions of the investigated region are: $x_{max} = 4$ μm and $y_{max} = 2$ μm. The number of mesh nodes is 1000 in each coordinate direction. The initial thickness of the oxide SiO_2 film always existing under real conditions and needed for starting the computational algorithm was taken to be equal to 4 mm (two mesh intervals). The initial distributions of the dopants B and P in Si were uniform and the concentration of the dopants was 10^{14} and 10^{15} cm^{-3}, respectively. Computer simulation cycles were carried out with variation in the process temperature T from 900 to 1250°C and in the oxygen O_2 pressure p from 0.9 to 1.2 atm. The value of the time step τ was chosen from the considerations of a compromise between the accuracy of the simulation (the oxidation wave in one time interval should pass through no more than two coordinate intervals) and the acceptable time of counting one variant (no more than 10 min for Pentium-4, processor of 2.8 GHz, bus of 800 MHz). The concrete value of τ strongly depends on the parameters p and T determining fast or slow oxidation. The solution process ended either upon the expiration of the given time or upon reaching the given maximum depth of penetration of the oxide into the base material along the vertical coordinate y or at the given value of $\Delta y = 0.3$ μm. Below the results of the simulation at $T = 1100$°C and $p = 1$ atm are presented.

Physico-Mathematical Formulation and Computational Algorithm for Solving the Problem of Crystalline Silicon Oxidation. One of the main segments of the technology of designing semiconductor materials with required electrophysical properties is the mask technology of conducting the process of oxidation of the base material substrate — a group IV chemical element of the Periodic table — Silicon Si (titanium Ti or germanium Ge) in which acceptor and donor dopants — group III and V chemical elements — boron B (gallium Ga or aluminum Al) or phosphorus P (antimony Sb or Arsenic As) are implanted. The aim of this stage of the MOS-technology is to create special, particular distributions of the concentrations of dopants in the silicon substrate, i.e., to form selectively highly doped regions (future drains and sources of transistors). Doping of parts of the monocrystalline silicon plate with atoms of different chemical elements in order to organize, in the silicon semiconductor, domains with n- and/or p-type conduction is carried out in a layer of specially created dielectric (silicon dioxide). Special protective masks covering a part of the silicon surface inhibit the process of its oxidation, and in the open parts the oxidation process can be very intensive.

The technical progress in the manufacture of multi-purpose semiconductor devices has led to a great demand for scientific investigations in this field, and in this connection it is impossible to give even a brief review of the existing works on all the above topics. At present the key problem causing the greatest difficulties is the simulation of the dynamics of motion of the oxidation wave boundaries in the base material and the segregation of dopants at its front. The quantum-mechanical approach to the solution of this problem faces great difficulties of constructing Hamilton operators for the Schrödinger equation and is practically unrealizable even on modern computing facilities. This leads to the necessity of using much simpler approaches in constructing approximate models for developing really functioning algorithms not only for 1D, but also for 2D (and even 3D) problems. Hereinafter the standard abbreviation of the dimensionality problem is used: one-dimensional — 1D, two-dimensional — 2D, and three-dimensional — 3D.

The physico-mathematical problem on the base material oxidation process is reduced to two basic subproblems on the dynamics of the oxide/oxidizer and oxide/material interfaces and on the growth of the oxide layer with its increasing and deforming volume.

The region of the investigated physical process (see Fig. 1) consists of three subregions: material Si, oxide SiO_2, and oxidizer O_2. Let these subregions be separated from one another by boundaries G_1 and G_2

$$G_1: \quad y = y_1(x, t), \quad SiO_2/Si, \tag{1}$$

$$G_2: \quad y = y_2(x, t), \quad SiO_2/O_2. \tag{2}$$

The boundary G_1 moves into the depth of Si, and G_2 moves into the subregion of O_2. In so doing, the condition

$$\Delta_1 = \alpha\Delta_2 \tag{3}$$

is imposed on their motion in addition to the laws of motion of fronts. This conditions is called "the volume growth law" and relates the volume Δ_1 of the substance that has reacted to the volume Δ_2 of the oxide that has arisen from it. In particular, to transform crystalline silicon Si into silicon dioxide, $\alpha = 4.4$ is needed. It should be emphasized that in some technological processes a part of the boundary G_1 can be covered with a protective mask inhibiting oxidation. The point of the simulation is to determine the evolution of the boundaries G_1 and G_2 with their possible self-intersection and the formation of multiply connected regions.

The approximate model used for the calculations is based on the replacement of the complex physicochemical description of the process by its averaged analog — the process of oxidizer diffusion through the oxide to the material with the use of a sufficiently empirical model of the interaction at the boundaries. The following evolution-boundary-value problem is stated: in the SiO_2 subregion a solution of the diffusion equation

$$\frac{\partial C}{\partial t} + \nabla\mathbf{F} = 0, \tag{4}$$

where the diffusion flow $\mathbf{F}$ is related to the diffusion coefficient D and the gradient of the oxidizer concentration C by the relation

$$\mathbf{F} = -D(x, y, C)\cdot\nabla C \tag{5}$$

is sought. The boundary conditions are determined by the equality of the diffusion flow (5) to the oxidizer flow through the boundaries in SiO_2:

$$G_1: \quad \mathbf{F} = \delta\cdot C\cdot\mathbf{n}_1, \tag{6}$$

$$G_2: \quad \mathbf{F} = h\cdot(C^* - C)\cdot\mathbf{n}_2. \tag{7}$$

Here δ, h, C^* are the physical constants of the problem (see, e.g., [2]), and $\mathbf{n}_1$ and $\mathbf{n}_2$ are normals to G_1 and G_2 respectively. System (4)–(7) is closed at the boundaries $x = 0$ and $x = x_{max}$ by the condition

$$\mathbf{F} = 0. \tag{8}$$

The velocity of motion $\mathbf{V}_1$ of each point of the boundary G_1 is determined by the velocity of penetration of the oxidizer into the material:

$$\mathbf{V}_1 = \frac{\mathbf{F}}{N}. \tag{9}$$

One can definitively determine by (9) the evolution of the boundary G_1. The evolution of the boundary G_2 is related to the evolution of the boundary G_1 only indirectly via condition (3), which is necessary but not sufficient for a definitive determination of the form and dynamics of G_2. This point in the given problem is the most difficult and requires special modeling.

The computer simulation of such a complex process faces great difficulties and is now reduced mainly to the solution of one-dimensional problems or 2D-simulation in the quasi-one-dimensional formulation, where in one of the coordinate directions direct numerical simulation is performed, and the influence of the second coordinate direction is taken into account by some empirically constructed analytical dependences. In this empirical approach, the "beak" model [2] and its numerous variations are most generally used.

To simulate the process of oxide film growth, the "compressible" model or the "pressure" model, the "viscous" model, and the "viscoelastic" model are used widely (see, e.g., [3–7]). The point of all these models is the representation of the physical process of oxide formation by a certain analog from the field of hydrodynamics, and the oxide therewith is considered as a liquid: as an incompressible and ideal liquid (without viscosity and heat conduction) in simple models, as a compressible and ideal liquid in other models, as a compressible and viscous liquid in third models; in fourth models, to describe the process as a hydrodynamic one, some notions from the theory of elasticity and plasticity are added. In these models, essentially artificial elements take place, such, e.g., as methods for constructing a "viscous stress tensor," determination of the transfer coefficient, as well as the closing of the hydrodynamic part of the system of equations by some analog of the equation of state establishing relations between "pressure," "density," and "temperature." These models are intended for solving variants of particular problems and, in fact, cannot be extended beyond their scope. This is evidenced by the very fact of the appearance of more and more intricate models for the hydrodynamic description: incompressible–compressible nonviscous — compressible viscous–compressible viscoelastic models.

In the present work, to simulate the evolution dynamics of the oxide layer, we used a specially designed computational method of "coherent (pairwise conjugate) points," relying (in some sense), in terms of methodology, on the ideology of the string theory. The salient point of this method is as follows. Each point of the SiO_2/Si interface is connected to one and only one point of the SiO_2/O_2 interface by some "virtual channel," a 1D-line (direction). It is assumed that along this line O_2 penetrates into Si through SiO_2, and in the reverse direction "diversion" of a part of the newly grown volume of SiO_2 takes place. The coherent point at the SiO_2/Si interface moves perpendicularly to its front for distance $d_1 = \mathbf{V}_1\mathbf{n}_1\tau$ on each step τ of the computational algorithm, and the velocity $\mathbf{V}_1$ is determined by the physics of the process — the velocity of penetration (9) of the oxidizer into the material.

The oxide layer growth on the opposite side occurs by the movement of the coherent point on the other end of the "virtual channel" at the SiO_2/O_2 interface perpendicularly to its front into the O_2 region for distance d_2 on each time step of the computational algorithm. This displacement is also determined by the physics of the process — by law (3) of oxide volume growth from the material $d_2 = d_1/\alpha$.

It should be emphasized that the "virtual channels" do not intersect, which excludes the nonphysical possibility of cross motion of the medium and oxidizer in the oxide.

In the algorithm, special methods have been developed for determining the coherence of the points of parts of SiO_2/Si and SiO_2/O_2 boundaries lying under protective masks, as well as method for organizing calculations in the case of the formation of multiply connected subregions of Si in SiO_2. The computational procedure, the algorithm and some features of its computer realization, and the results of computing experiments are described in detail in [8].

Physico-Mathematical Formulation and Computational Algorithm for Solving the Problem of Segregation of Dopants. The basic element of this technological stage, called "base substrate annealing," relies on the special effect — the fact that at the SiO_2/Si oxidation wave front segregation of dopants B and P occurs. Segregation is a complex physicochemical process in which special properties of the action of the oxidation wave front of a group IV material on acceptor and donor dopants of group III and subgroup V (a) (of the type of B and P respectively) implanted in this material manifest themselves. Dopants of the type of P are forced out of the oxide into the material, and B-type dopants, vice versa, are drawn from the material into the oxide with subsequent diffusion in Si and SiO_2 and convective transfer in SiO_2.

The last process is associated with the "growth" of the SiO_2 volume from Si, since a unit volume of Si yields about 2.27 volumes of SiO_2 with a corresponding growth of the oxide film into the region of the oxidizer O_2 (into free space).

The redistribution of dopants and their resulting configuration create the required electrical semiconductor properties of the material. It should be noted that to simulate one of the processes of charge transfer in semiconductors, the "hydrodynamical" model of the bullistic diode [6, 7] is used quite successively.

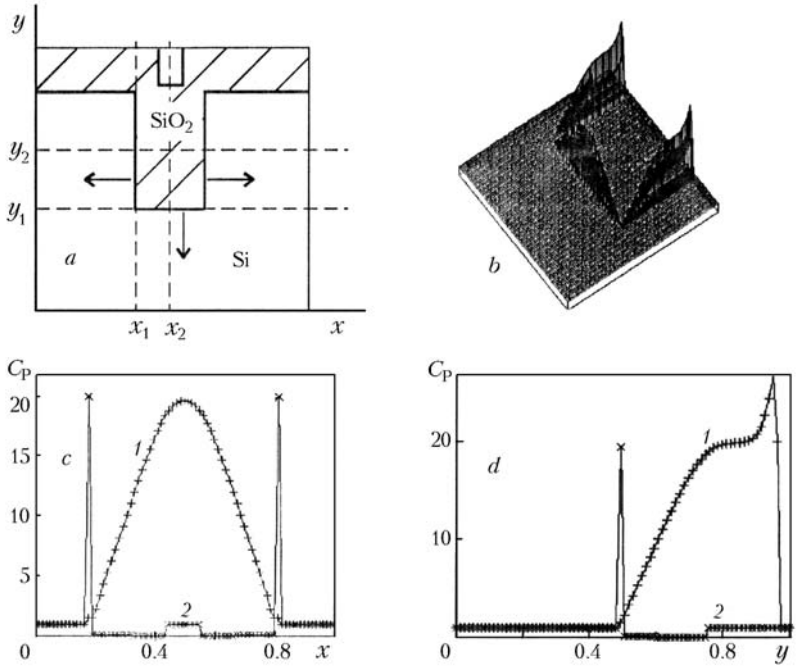

Fig. 2. Segregation of the dopant phosphorus in silicon at the oxidation wave front: redistribution of the concentrations of P in Si.

Modeling the segregation phenomenon at a high level (quantum mechanics, statistical physics) requires too large computational resources, therefore significantly averaged approaches are used. The essence of the approximate model is as follows. The "oxide/material" wave, which is considered as an infinitely fine discontinuity, moving into the depth of the material, established at each point of its front (along the normal to it) the relation called the segregation law:

$$m = \frac{C_+}{C_-}, \tag{10}$$

where C_+ and C_- are dopant concentrations in the base material before the front and in the oxide behind the discontinuity front, respectively. The quantity m approximately depends on a number of factors

$$m = m_0 \exp(-W/kT), \tag{11}$$

where m_0 is a pre-exponential factor. The values of m_0 and W are significantly different for different chemical elements and are determined by a particular type of dopant in the interaction with a particular type of wave. Relation (11), generally speaking, holds for equilibrium processes. However, a nonequilibrium correction can be introduced into the given hypothesis of the infinitely fine discontinuity (10) (for more detail see [2, 9]).

The solution of problem (10), (11) in the 1D-formulation presents no special difficulties. However, extending approach (10) to a 2D- and, the more so, to a 3D-problem, is frought with great difficulties, including those connected with passing from a continuous differential problem to a discrete one, especially in complex modeling of the complete problem in general (oxidation of the material, segregation of the dopants, evolution of the oxide layer, diffusion of the dopants in the oxide and material, etc.).

Correct decomposition of the complete problem and sequential calculation of its individual segments permits, in our opinion, more effective simulation of complex physical processes. In [9], a detailed description of the developed effective computational algorithm for solving the problem on the segregation of dopants of different types (acceptor and/or donor ones) at the oxidation wave front is presented, as well as relevant bibliography is given. The key aspects of this algorithms are described in detail. These are: triangulation of the calculation domain, determination of the direction of forcing-out or drawing-in of dopants, calculation of the mass forced out of the cell-donor, calculation of the

masses received by cells-percipients, control over the mass conservation of dopants. The results of computing experiments on the segregation processes are presented in [10, 11].

To illustrate the effects of segregation and analysis of the "sources" of the appearance of nanostructures of dopants determining the special electrophysical properties of a material, Fig. 2 shows the results of the model problem solution (segregation in "pure" form without the diffusion "smearing" of the segregation peaks of the dopant concentration distribution).

Figure 2a shows the scheme of the problem. In the region of the base material Si of size 1 μm × 1 μm the region of the oxide SiO_2 in the form of a "trench" develops. At the initial instant of time this region was represented in the form of a narrow slot $0.75 < y < 1$ at $x = 0.5$. By the instant of time under consideration the region of SiO_2, moving into the depth of Si (in different directions indicated by arrows), has reached the position (shaded part): the "trench" bottom — the coordinate $y_1 = 0.5$, the left wall — the coordinate $x_1 = 0.2$. The whole picture of the process is mirror-symmetric with respect to the middle line $x = 0.5$.

At the initial instant of time the phosphorus concentration C_P throughout the region was uniform and equal to 1000 μm^{-3}. Normalization to this value has been performed. Figure 2b illustrates the resulting (isothermal) C_P distribution pattern that arises by the time $t_{max} = 20$ min. In the calculations, we used a uniform mesh of 1000 × 1000 nodes with a width of 1 nm in each direction; the computer time of the calculation was 20 sec for a Pentium-4 with a clock frequency of 2.8 GHz and a bus of 800 MHz. One can readily see the steep "walls" of the segregation front actually coinciding with the position of the SiO_2/Si front, which have formed a new cavity. From this cavity an appreciable part of P was forced out outside into Si before the SiO_2/Si front. At the corners of the cavity, the value of the "wall" $C_P(x, y)$ is much less than at the centers of the leading, left, and right fronts, illustrating the effect of a "bulldozer" when on the blade of this road-building mechanism the cut ground forms a characteristic configuration with a maximum at the center and a minimum at the edges.

Figure 2c shows the $C_P(x, y)$ distribution along the x-axis at two fixed values: $y_1 = 0.5$ and $y_2 = 0.7$ (curves 1 and 2 respectively). Their positions in the problem are marked in Fig. 2a by dashed lines. The following distribution of concentrations takes place. In the region of the material Si ($x < 0.2$ and $x < 0.8$), the initial values of $C_P(x, 0.5) = 1$ and $C_P(x, 0.7) = 1$ are preserved. Directly at the SiO_2/Si front ($x = 0.2$ and $x = 0.8$) there occurs a stepwise increase in $C_P(0.2, 0.7)$ to values of 20 and an even more significant decrease immediately behind the front on an interval of only about 10 nm to 0.1 in the oxide region corresponding to the segregation law (10): $C_+/C_- = 20/0.1 = 200$.

The slight increase in the C_P values at the center of the region $0.45 < x < 0.55$ at $y = 0.7$ (curve 2) represents a trace of the downward movement of the horizontal part of the "trench" in the vertical direction. For the distributions at $y = 0.5$ (curve 1), in the segment $0.2 < x < 0.8$ passing along the SiO_2/Si front on the bottom of the cavity, the values of $C_P(x, 0.5)$ smoothly increase from 1 at $x = 0.2$ to 20 at $x = 0.5$ (at the central point of the bottom).

Figure 2d illustrates two one-dimensional distributions of $C_P(x, y)$ along the lines $x_1 = 0.2$ (along the left front SiO_2/Si) and $x_2 = 0.5$ (the central line of the problem) given, respectively, by curves 1 and 2. As in the foregoing, the initial distribution of C_P in Si, a sharp jump before the SiO_2/Si front, and as sharp a drop behind the front in the SiO_2 region take place (curve 2). The increase in the concentration C_P directly along the SiO_2/Si front (curve 1) has a smooth character with an increase from 1 from the "trench corner" at the point (x_1, y_1) to about 30 at the point (0.2, 0.9). Thus, the one-dimensional graphs in Fig. 2c and d numerically detail the spatial pattern of Fig. 2b.

The developed computing algorithm for calculating segregation problems has demonstrated a high accuracy and no-failure functioning in a wide range of diagnostic variables and is one of the key aspects (see [12–14]) of computer design of semiconductor materials with given electrophysical properties.

Dynamics of the Oxide Film Boundaries. After analyzing the results of the solution of the model problem (in which the segregation processes of phosphorus in silicon were considered at the front of motion of some arbitrary boundary) we turn to the analysis of the results of solving the formulated physicochemical problem (Fig. 1) with real parameters (pressure, temperature, etc.) of this technological segment (annealing) of the production cycle. Figure 3 shows the time evolution of the configurations of the SiO_2/Si and SiO_2/O_2 fronts, reflecting the dynamics of movement of the oxidation wave into the material (into the region of decreasing y) and extension of the oxide towards the oxidizer (into the region of increasing y). Each line of these "congruent," in a sense, nonintersecting curvilinear curves shows the position of the corresponding boundary at some instant of time t, from $t = 0$ (central line) to $t = t_{max}$, at

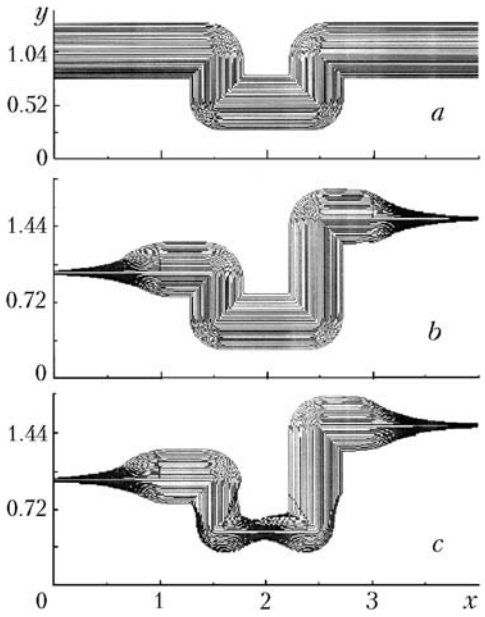

Fig. 3. Growth dynamics of oxide (silicon dioxide SiO_2) film with time in the process of annealing silicon Si plates in oxygen O_2 for three initial configurations of the material surface: without protective masks (a); with two (b) and three (c) protective masks.

which the given oxidation depth has been reached. The curves are equitemporal, i.e., representing the position of the boundaries at regular intervals, and pairwise matched: to each curve of the lower family (SiO_2/Si boundary) there corresponds a curve of the upper family (SiO_2/O_2) given for this same instant of time. The extreme upper and lower curves represent the resulting boundaries of the oxide film at the final instant of time.

Analyzing the dynamics of the curves (see Fig. 3), we can determine the influence of masks on the oxidation rate not only qualitatively but also quantitatively and follow the development of the initially flat oxide film into a "beak" configuration [2] with a strong compression of the family of curves under masks. Unlike [2], the result presented was obtained immediately by direct numerical simulation without using the "adjustable parameters" characteristic of the "beak" model: "thickness and slope of the beak," "shift" of the edge of the mask, etc. The model of [8] does not need such parameters, and the shifts of the mask edges and their bends are determined in the calculations exactly from the principle of "mask length invariance at bending" by integrating the distance along the mask surfaces. Moreover, the developed model makes it possible to investigate situations where the regions of influence of masks close and at SiO_2/Si and SiO_2/O_2 interfaces flat portions are absent altogether; these situations cannot be simulated with the use of analytical methods of the type of [2]. Note also that integral control over the procedure of calculating the dynamics of boundaries with a significant lift of the system of masks by the growing oxide film determined by the "volume growth" law (the oxide volume equals 2.27 of the material volume) points to a good accuracy of the process simulation.

The theoretical model, the solution method, the computational algorithm, the features of the computer programs, and multiaspect numerical experiments are described in detail in [8–11].

Below we consider the results of the mathematical modeling of the given problem. Note an important peculiarity (Fig. 3) of the form of the grown silicon dioxide, which cannot be obtained with the use of the models of [2–5]. Noteworthy are the right angles of the Si/O_2 interface, whose vertices prior to the beginning of the oxidation process had coordinates (1.5, 1) and (2.5, 1) for the variant of Fig. 3a and (1.5, 1) and (2.5, 1.5) for the variants of Fig. 3b and c, respectively.

The time evolution of these angles upon splitting of the Si/O_2 interface occurs differently for the "oxide/oxidizer" SiO_2/O_2 interface (upper bound of the oxide) and the "oxide/material" SiO_2/Si interface (lower bound). For the SiO_2/O_2 boundary, these angles deform significantly, and for the SiO_2/Si interface the angles retain the practically

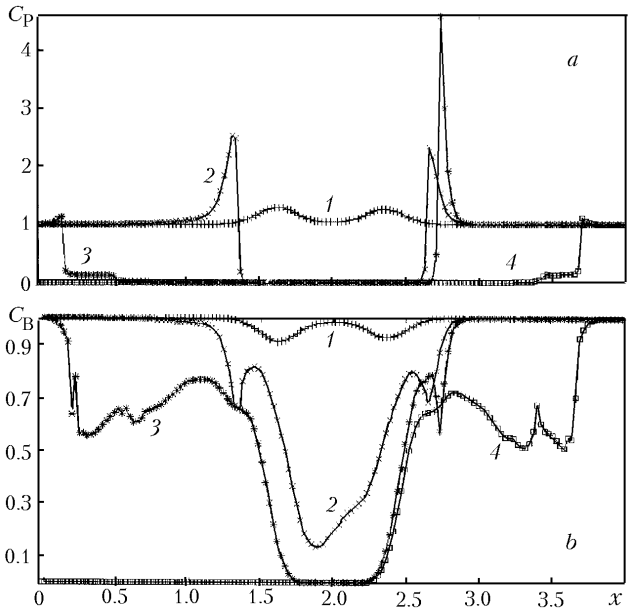

Fig. 4. Distribution of the concentrations of phosphorus C_P (a) and boron C_B (b) in silicon and silicon dioxide along x at various values of y = 0.20 (curve 1), 0.61 (2), 1.0 (3), and 1.47 (4) for the three-mask annealing technology.

rectangular form except for the three-mask variant (Fig. 3c), where the bottom mask redistributes the O_2 flows in SiO_2 to Si, which strongly influences the form of the SiO_2/Si interface, including the rectangular form of the portion. Note that the different evolution of the right angles of the "oxide/oxidizer" and "oxide/material" interfaces is determined by the essentially different mechanical properties of Si (crystal lattice, hardness of the material) and SiO_2 (amorphism, viscoelastic properties).

The evolution of the other angles of the "trench" with initial coordinates (1.5, 0.5) and (2.5, 0.5) has a different character. These angles are exterior ("obtuse") for the material and equal 270^o unlike those considered above, where the angles for the material were interior ("acute") with right angles of 90^o. Upon "splitting" of the Si/O_2 interface the rectangularity is preserved for the SiO_2/O_2 interface, and at the SiO_2/Si interface they transform significantly. The mask covering part of the trench bottom influences the rectangularity of the left wall to a greater extent than of the right one because of their different height. Note also that by the end of the process the left wall has lost its flat form, and the right wall preserves its flat surface in a large part.

The form of the SiO_2/Si interface (and to a lesser extent of the SiO_2/O_2 interface) radically influences the final distribution of the concentrations of dopants and the formation of their special nanostructures (see also [10, 11]). Note that certain features of the hyperfine film dynamic at the initial stages of the process, at small values of t, when the silicon dioxide thickness is less than 50 nm, are modeled by the computational algorithm [9] with a sufficient accuracy (see also [4]).

Formation of Nanostructures of the Dopants. On completion of this technological stage, when as a result of the substrate annealing the oxidation wave front has moved on the "trench" bottom into the depth of the material for 200 nm, the uniform (at the initial of time) distributions of the concentrations of the dopants phosphorus $C_P(x, y)$ and boron $C_B(x, y)$ become essentially nonuniform as a consequence of the segregation process. In the silicon substrate, special nanostructures — narrow-localized regions with very high values of C_P and C_B, i.e., regions with high, respectively, electron (n-type) and hole (p-type) conductions — have formed. This provides, in the following technological stages, organization of sources and drains of transistors and their channels and gates.

Below we analyze the results of the computer simulation of the three-mask variant of annealing shown in Fig. 3c.

Figure 4 gives the distributions of the concentrations of phosphorus $C_P(x, y)$ and boron $C_B(x, y)$ in silicon and silicon dioxide along x at various values of y. These coordinates are highly characteristic horizontal levels of the prob-

lem. The level $y = 0.20$ is a horizon reached by the oxide wave in the central part moving downward from the "trench" bottom (see Fig. 3). On the right and left the substrate of the nonoxidized material is given. Accordingly, here $C_P(x, 0.20) = 1$ and $C_B(x, 0.20) = 1$. The values of the concentrations have been normalized to their initial values. But on this horizon under the "trench" bottom in the subregion ($1.5 < x < 2.5$), the curves of the concentrations C_P and C_B have a wavy character — cosine-shaped (with a maximum at the center of the subregion $x = 2$) for C_B and sine-shaped (with a maximum at the center) for C_P. Such a combination of the C_P and C_B configurations enhances the conductor properties (of the n- and p-type) with the possibility of organizing here of a current reverser in the channel.

The level $y = 0.61$ is a horizon inside the Si region on the left and right of the "trench" crossing the region of maximum formation of oxide in the "trench." This horizon is an internal line in the material Si along which SiO_2/Si the oxidation wave moves from the right wall of the trench to the right boundary of the calculated region. At this level the evolution of SiO_2/Si motion leads to a significant redistribution of the concentrations along the x-direction. For phosphorus (curve 2, Fig. 4a), the initial distributions of $C_P = 1$ are preserved up to $x \approx 1.2$. Then, before the SiO_2/Si front ($x \approx 1.35$), there occurs only a sharp increase in C_P up to 2.2 and an even sharper decrease behind the front, practically to zero in the region of the oxide SiO_2 ("bulldozer" effect with almost complete forcing out of the phosphorus dopants, see also [11]). Then, after the rather extended region of SiO_2 with a practically zero concentration of phosphorus, there occurs an even sharper increase in C_P from 0 to the value of 4.5 at the SiO_2/Si front on the right of the trench at $x \approx 2.7$ followed by a decrease in the subregion of $x > 2.8$ (in Si) to the initial values of $C_P = 1$. It should be emphasized that these sharp increases are narrowly-localized with a band width of about 60–80 nm.

The distribution of boron concentrations $C_B(x, 0.61)$ is considerably different (curve 2, Fig. 4b). On the left, in the subregion of $x < 1.2$ (in Si) the values of $C_B = 1$. Further, before the SiO_2/Si front ($x \approx 1.35$) C_B sharply decreases and the concentration behind the front increases ("vacuum cleaner" effect, see also [10]). However, in the region of the oxide SiO_2 there is again a decrease in C_B with a deep minimum of $C_B \approx 0.15$ at the point $x \approx 1.9$. This is due to the strong diffusion of the dopant B in SiO_2, as well as to the proper motion of the oxide and, accordingly, to the convective transfer and the redistribution of the dopant B. At the right boundary of the "trench" the C_B distribution is analogous, with a small maximum of 0.8 behind the front ($x \approx 2.7$), a minimum of 0.7 before the front ($x \approx 2.8$) of SiO_2/Si, and a return to the initial value of 1 in the subregion of Si ($x > 2.9$).

The level $y = 1$ is a horizon of the left surface of the silicon plate at the initial instant of time where the dominant direction of the oxidation process is the vertical and (additionally, from the left wall of the "trench") horizontal direction. This level crosses the "trench" boundary, where only the horizontal direction dominates in the oxidation process. The results of the redistribution of dopants P and B at this level are presented by curves 3 in Fig. 4a and b, respectively. The dependence $C_P(x, 1)$ has a simple form, and the form of $C_B(x, 1)$ is more complicated and is determined by the interference of the processes analyzed above in detail for the levels 0.20 and 0.61. Note that almost the whole of the phosphorus has been forced out of the oxide subregion. To ensure against incorrect analysis, it will be recalled that at this level (see Fig. 1 and Fig. 3c) there exist five subregions: of Si (partly under a mask), SiO_2, O_2, SiO_2, and Si (enumeration from left to right along x). Naturally, in the O_2 region the dopant concentrations are zero.

The level $y = 1.47$ is given in Fig. 4a and b for the analysis of two almost independent processes: motion of the vertical front of SiO_2/Si in the horizontal direction from the right wall of the "trench" and motion of the horizontal front of SiO_2/Si in the vertical direction (with the penetration into the horizontally positioned mask). The SiO_2/O_2 fronts move in opposite directions.

The analysis performed above should be complemented by an investigation of the distribution of phosphorus and boron concentrations obtained by the end of the annealing process in the y-direction transverse to the surface of the Si plate.

Figure 5a and b shows, respectively, the distributions of the concentrations of phosphorus $C_P(x, y)$ and boron $C_B(x, y)$ in silicon and silicon dioxide along y at various values of x. These vertical lines transverse the most characteristic zones. The first line passes through the regions of the material Si, crosses the SiO_2/Si and SiO_2/O_2 fronts (between which the SiO_2 subregion is situated) and goes into the O_2 region. The second line is the central line of the problem. It starts in the Si region, crosses the mask lying on the bottom of the "trench," around which a fairly thick

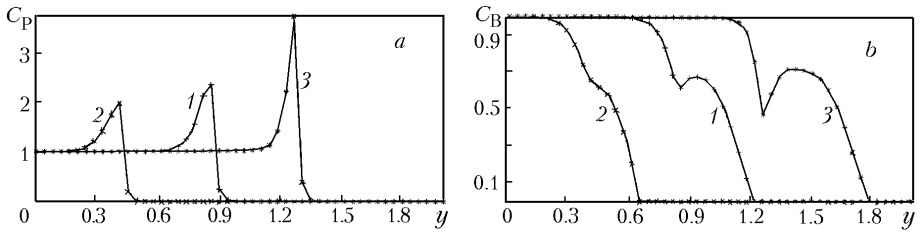

Fig. 5. Distribution of the concentrations of phosphorus C_P (a) and boron C_B (b) in silicon and silicon dioxide along y at various values of x = 0.75 (curve 1), 2.00 (2), and 2.90 (3) for the three-mask annealing technology.

SiO_2 layer has formed, and goes into the O_2 region. The third line is adequate to the first one with the only difference that it passes in a higher layer of Si (on the right of the "trench").

Let us analyze the resulting distribution of the dopant phosphorus along the central line of the problem (curve 2, Fig. 5a). If the mask covered the whole of the "trench" bottom, then the distribution of $C_P(2, y)$ would remain till the end of the process equal to unity under the mask (in Si) and zero in O_2. In the given production cycle, where the mask is twice shorter than the width of the "trench," the oxidation process (SiO_2/Si front) moves also under the mask. In so doing, the front "pushes" ahead the phosphorus and "draws" the boron in. Since the oxidation wave fronts moving under the center of the mask from its left and right edges have closed at the level $y \approx 0.4$ (see Fig. 3c), one would expect a maximum here, which just happens: $C_P(2, 0.4) \approx 2$. Next, with increasing $y > 0.5$, a region over the mask is formed (at t = 0 here C_P = 0). At the moment of completion of the process over the mask a region of the oxide SiO_2 up to $y \approx 0.6$ is formed. Now the concentration C_P is very insignificant here, but nevertheless it is not zero (residual "underpushing" of P into SiO_2). The oxide dislocation over the mask is determined by the law of "growth" of the SiO_2 volume from Si and the motion of SiO_2 above the mask from under it and from the "trench" walls.

The distribution of phosphorus on the other lines is basically analogous (curves 1 and 3, Fig. 5a). A C_P maximum is formed near the SiO_2/Si front with a smooth change to the region of Si and a sharp drop to the region of SiO_2, and then to zero values in the region of O_2.

The distributions of boron concentrations C_B formed on these verticals are more complex (see Fig. 5b) due to the fact that B is not pushed into the oxide as P, but is drawn into it from the silicon regions closest to the SiO_2/Si front with a further redistribution inside SiO_2 because of the diffusion and convective mixing in the oxide. Nevertheless, in Fig. 5b one can locate the oxidation wave front by the characteristic mark — the nearby local minimum and maximum of C_B. This is well illustrated by curves 1 and especially 3, where the influence of protective masks is not dominant in the process of redistribution of the dopants.

Thus, in the process of redistribution of the oxidation waves in the base material the uniform (at the initial instant of time) distributions of the dopants phosphorus and boron have become essentially nonuniform along each coordinate direction because of their segregation at the SiO_2/Si front.

Conclusions. Mathematical modeling of the physicochemical processes underlying one of the segments of the technological cycle of making new semiconductor materials for nanoelectronics has been performed. This production stage — annealing of the base material (Si, Ti or Ge) substrate — is intended for forming special nanostructures of donor (P, As or Sb) and acceptor (B, Ga or Al) dopants uniformly distributed in the base material before the beginning of annealing. In this work, for one variant of configurations of the substrate surface ("trench") partly covered by protective masks preventing the action of the oxidizer on parts of the surface, we have investigated the growth dynamics of the oxide film and studied the dopant redistribution resulting from the physicochemical process of segregation at the "oxide/material" wave front. We have obtained and analyzed the distributions of dopant concentrations with the formation of various domains, including the specific nanostructures — narrow-localized zones (of size 40–60 nm) with a higher concentration of donor and acceptor dopants. In these zones, because of the high electron (n-type) and hole (p-type) conduction, it is possible to organize, upon realizing the other technological stages of production, diode and transistor channels, as well as other elements of integrated circuits. The width of these nanostructures determines the packing density of crystal transistors. Increasing the accuracy of modeling with two main lines — by using physicomathematical models more adequate to the real physical processes and employing parallel technologies of high-effi-

ciency calculations on supercomputers — will make it possible to considerably improve the characteristics of integrated circuits being developed.

The author wishes to thank prof. S. N. Korobeinikov for helpful discussions.

This work was supported by the Russian Foundation for Basic Research (project No. 06-08-00384).

NOTATION

C, concentration of dopants, cm^{-3}; d, displacement of the front in each step of the computational process; D, diffusion coefficient; **F**, diffusion flow of the dopant concentration; h, coefficient of diffusion penetration of the oxidizer into the material; k, Boltzmann constant; m, segregation coefficient; **n**, normal to the boundary surface of oxide; N, number of oxidizer molecules required for the formation of a unit volume of oxide; p, pressure, atm; t, time, min; T, temperature, ^{o}C; **V**, local velocity of motion of the oxide boundary; W, segregation potential; x, y, Cartesian coordinate system μm; α, coefficient of oxide growth from the material; δ, coefficient of diffusion penetration of the oxidizer into the oxide; Δ, volume of the oxide formed; τ, value in the time step algorithm, μsec. Subscripts: max, maximum value; 0, equilibrium value; 1 and 2, parameters at the "oxide/material" and "oxide/oxidizer" interfaces; *, nonequilibrium value.

REFERENCES

1. S. A. Pakhomov, Revolution in the production of transistors, *Computer Press*, No. 1, 76–83 (2004).
2. B. E. Deal and A. S. Grove, General relationship for the thermal oxidation of silicon, *Appl. Phys.*, **36**, 37–70 (1965).
3. C. P. Ho and J. D. Plumber, Si/SiO_2 interface oxidation kinetics: a physical model of high substrate doping levels, *J. Electrochem. Soc.*, **126**, No. 9, 1516–1522 (1979).
4. A. Ya. Vul', T. L. Makarova, V. Yu. Osipova, Yu. S. Zinchik, and S. K. Boitsov, Kinetics of silicon oxidation and the structure of oxide layers of thickness less than 50 Å, *Fiz. Tekh. Poluprovodn.*, **26**, No. 1, 111–121 (1992).
5. V. Senez, P. Fereiza, and A. Baccus, Two-dimensional simulation of local oxidation of silicon: calibrated viscoelastic flow analysis, *IEEE Trans. Elec. Dev.*, **43**, No. 5, 720–731 (1996).
6. V. Romano, 2D simulation of a silicon MESFET with a nonparabolic hydrodynamical model based on the maximum entropy principle, *J. Comput. Phys.*, **176**, No. 1, 70–92 (2002).
7. A. M. Blokhin, R. S. Bushmanov, and V. Romano, Asymptotic stability of the equilibrium state for the hydrodynamical model of charge transport in semiconductors based on the maximum entropy principle, *Int. J. Eng. Sci.*, **42**, No. 8–9, 915–934 (2004).
8. A. L. Aleksandrov, G. A. Tarnavskii, S. I. Shpak, A. S. Gulidov, and M. S. Obrekht, Numerical simulation of the problem of the dynamics of oxide film growth in semiconductor substrates on the basis of the geometric approach and the Deal–Grow method, *Vychisl. Metody Programmir.*, **2**, No. 1, 92–111 (2001).
9. G. A. Tarnavskii, S. I. Shpak, and M. S. Obrekht, Numerical simulation and computer algorithm of the process of segregation of dopants at the oxidation wave boundary in semiconductor substrates, *Vychisl. Metody Programmir.*, **2**, No. 1, 12–26 (2001).
10. G. A. Tarnavskii, S. I. Shpak, and M. S. Obrekht, Segregation of boron implanted in silicon on angular configurations of the silicon/silicon dioxide oxidation wave, *Pis'ma Zh. Éksp. Teor. Fiz.*, **73**, No. 9–10, 536–541 (2001).
11. G. A. Tarnavskii, S. I. Shpak, and M. S. Obrekht, Features of the segregation of dopants of V(a) subgroup elements on angular configurations of the silicon/silicon dioxide oxidation boundary, *Inzh.-Fiz. Zh.*, **75**, No. 1, 142–147 (2002).
12. G. A. Tarnavskii, A. V. Aliev, and A. G. Tarnavskii, Mathematical modeling of the processes of formation of nanostructures of dopants in the base material (nanotechnologies for microelectronics), *Sib. Zh. Vychisl. Mat.*, No. 4, 401–416 (2007).

13. G. A. Tarnavskii, A. V. Aliev, and A. G. Tarnavskii, Creation of special nanostructures of donor and acceptor impurities in the base silicon substrate for designing new semiconductor materials, *Nano-Mikrosist. Tekh.*, No. 9, 2–7 (2007).
14. G. A. Tarnavskii, A. V. Aliev, and A. G. Tarnavskii, Formation of nanostructures of donor and acceptor impurities upon annealing of the base silicon substrate, *Nanotekhnika*, No. 4 (12), 53–58 (2007).